Ab–initio study of the electronic and optical traits of Na$_{0.5}$Bi$_{0.5}$TiO$_3$ nanostructured thin film

Mohammadreza Askaripour Lahiji[*,1], Ali Abdolahzadeh Ziabari[2]

[1] Department of applied mathematics, Astaneh Ashrafieh Branch, Islamic Azad University, Astaneh Ashrafieh, Iran

[2] Nano Research Lab, Lahijan Branch, Islamic Azad University, P.O. Box: 1616, Lahijan, Iran

Abstract: The electronic, and optical properties of rhombohedral Na$_{0.5}$Bi$_{0.5}$TiO$_3$ nanostructured thin film have been studied by the first–principle approach. Density functional theory (DFT) has been employed to calculate the fundamental properties of the layers using full–potential linearized augmented plane–wave (FPLAPW) method. A 2×2×1 supercell was constructed with two vacuum slabs on top and down of the supercell. A geometry optimization was performed by PBE method. The optimized thin film structure was used for the intended calculations. As well, the reflectance, dielectric function, refractive index, of the thin film were calculated in the UV–vis region. Results showed very well consistency with the available experimental and theoretical reports. The optical conductivity also followed a similar trend to that of the dielectric constants. Energy loss function of the modeled compound was also evaluated. The evaluated loss function showed sharp peaks in UV-vis region and followed a steady state in IR, MIR and FIR parts of spectrum.

1. INTRODUCTION

Na$_{0.5}$Bi$_{0.5}$TiO$_3$ (NBT) is a relaxor perovskite (ABO$_3$) complex that shows ferroelectric and piezoelectric properties. ABO$_3$ has two different ions (Na and Bi) at the A site. Due to its potential to be used in electromechanical actuators, sensors, and transducers it has attracted many attentions as an appropriate Pb-free ferroelectric material [1]. It is also an appropriate candidate for energy storage [2]. Nowadays, energy storage materials have an intense area of research due to their wide application range in modern devices like power electronics, pulsed power systems, etc. Besides, the NBT has unusual phase transitions from the cubic $Pm\overline{3}m$ at temperatures above 813 K, to the tetragonal

---

* Corresponding author. Email: m.a.lahijiii@gmail.com

P4bm between 783 and 813 K, and to the rhombohedral *R*3c structure below 517 K, that implies peculiar dielectric and ferroelectric properties [2-4]. Regarding relatively large conductivity and large coercive field, the NBT ceramic is hard to be poled and its piezoelectric properties are not desirable. Instead, NBT single crystal presents desirable piezoelectric characteristics and premiere optical properties [5,6]. Mohanty et al calculated the energetic and structural properties of bulk $(NBT)_{1-x}$-$(BT)_x$ at x=0.0 and 12.5% with DFT method. In x=0.0% composition case, their calculations predicted that the rhombohedral *R3c* phase is the ground state of the system [3]. Niranjan et al used a combination of DFT analysis and experimental characterization to understand the lattice dynamics, dielectric and ferroelectric properties of lead–free relaxor ferroelectric $Na_{0.5}Bi_{0.5}TiO_3$ system [6]. They found that the Born effective charges of Bi and Ti ions are significantly larger than their nominal charges, particularly in direction perpendicular to the 3-fold [111] symmetry axis. Dorywalski et al prepared ultra-thin NBT films on (001) $SrTiO_3$ substrate by pulsed laser deposition technique [7]. They also calculated the band structure and density of states of the materials by DFT method. An indirect bandgap equal to 2.81eV was achieved for the simulated bulk NBT. Further survey in the literature reveals that reports on the DFT calculated optical properties of NBT particularly in the form of thin film are very scarce. However, NBT single crystal has been grown by different growth techniques [5,6] the fundamental study on its electronic structure and optical properties especially in the form of thin film is seriously limited. In this study, the electronic and optical properties of $Na_{0.5}Bi_{0.5}TiO_3$ nanostructured thin film have been studied by using first–principles calculations based on DFT as implemented in DMol^3 package [8].

2. COMPUTATIONAL DETAILS

The electronic and optical properties of $Na_{0.5}Bi_{0.5}TiO_3$ thin film are studied using a 2×2×1 $Na_{0.5}Bi_{0.5}TiO_3$ supercell as plotted in Fig. 1.
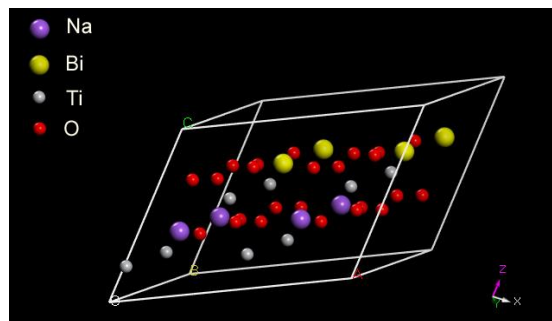
Fig. 1. The side view of the optimized structures of 2×2×1 structures of $Na_{0.5}Bi_{0.5}TiO_3$ nanostructured thin film.

A $Na_{0.5}Bi_{0.5}TiO_3$ (001) slab surface model is built using the supercell approach, which includes 1 layer of $Na_{0.5}Bi_{0.5}TiO_3$ atoms and two vacuum of 10 Å upper and bottom of the slab.

For the structural optimization, different exchange–correlation functional within local density approximation (LDA) and generalized gradient approximation (GGA) were tested, and the Hamprecht–Cohen–Tozer–Handy (HCTH) functional [9] at GGA level was opted for calculations. This method can perform accurate and efficient self–consistent calculations using a rapidly convergent three–dimensional numerical integration scheme. The basic functions were explained by a double numerical and polarized (DNP) basis set,

TABLE I

Optimized structure parameters for R3c $Na_{0.5}Bi_{0.5}TiO_3$ with a=0.557 nm α=59.6830°. The experimental values [10] are given in parentheses with a=0.551 nm and α=59.8028°.

Atom	x	y	z
Na/Bi	0.2705	0.2705	0.2705
	(0.2627)	(0.2627)	(0.2627)
Ti	0.0119	0.0119	0.0119
	(0.0063)	(0.0063)	(0.0063)
O	0.2060	0.2091	0.7495
	(0.2093)	(0.2093)	(0.7473)

and the global orbital cutoff was set to 4.4 Å. A Fermi smearing of 0.01 Hartree is used to enhance computational performance. The Brillouin zone integration is performed according to the Monkhorst–Pack [10] scheme with a grid spacing of 0.05 Å^{-1}(i.e. a $3 \times 3 \times 1$ k–points setting). A convergence accuracy of 1×10^{-5} Ha is used for the self-consistent field (SCF) calculation. No point group symmetry constraints are imposed in the calculations. The structural parameters, like the equilibrium lattice constants were calculated by performing structural optimization and the obtained values are summarized in Table 1. These results are very close to those found experimentally and theoretically by the other researchers [7, 11].

3. RESULTS and DISCUSSION

Fig. 2 displays the calculated band structure of R3c $Na_{0.5}Bi_{0.5}TiO_3$ thin film showing high-symmetric directions in the Brillouin zone. It is evident that the top of valence band and the bottom of conduction band are both located at the same point. Hence, a direct band gap is formed and the value is about 2.1 eV, which is consistent well with the literature [12]. Total density of states (DOS)

was also shown in Fig. 2. In the valence band, bands above -5 eV are related to the O 2p, Ti 3d, and Bi 6p states, that indicate a strong hybridization among them. In the conduction band, the bands between 2.1 and 7.7 eV are primarily related to Ti 3d, Bi 6p, and Na 2s states plus the hybridized O 2p states. It is necessary to say that the O 2p states are on the top of the valence band while the Ti 3d and Bi 6p states are located at the bottom of conduction band. Therefore, the electrical and optical features of $Na_{0.5}Bi_{0.5}TiO_3$ are regarded to be characterized by the charge-transfer transitions from O 2p to Ti 3d or Bi 6p states.

To investigate the optical properties of the modeled NBT thin film, the dielectric function ε, refractive index n, extinction coefficient κ, optical conductivity σ, reflectivity R, and energy–loss functions L were calculated.
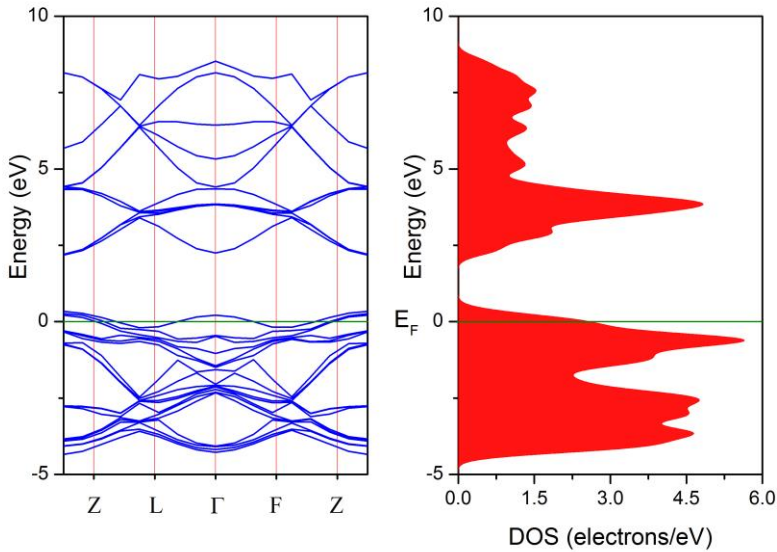
Fig. 2. The calculated band structure of NBT thin film along with the related total DOS.

The dielectric function (ε) can be expressed by the band–to–band transition, and its real ($\varepsilon_r(\omega)$) and imaginary ($\varepsilon_i(\omega)$) parts can be derived from the well-known Kramers–Kronig dispersion equations

$$\varepsilon_r(\omega) = 1 + \frac{2}{\pi} P \int_0^\infty \frac{\omega' \varepsilon_i(\omega')}{\omega'^2 - \omega^2} d\omega' \tag{1}$$

$$\varepsilon_i(\omega) = -\frac{2\omega}{\pi} P \int_0^\infty \frac{\varepsilon_r(\omega')-1}{\omega'^2 - \omega^2} d\omega' \qquad (2)$$

Fig. 3 shows a schematic overview of the dispersive part $\varepsilon_r(\omega)$ and the absorptive part $\varepsilon_i(\omega)$ of NBT nanostructured thin film calculated by GGA–HCTH. As it comes from the figure, the first leap of the spectrum occurs around 500 nm corresponding to the transition between VBM and CBM. The real part of dielectric function conveys a dispersive behavior while the imaginary part explains an absorptive characteristic of the material. Except the mentioned band-to-band transition region (i.e. around 500 nm), both parts show an increasing trend and the absorptive share is larger than the dispersive one.

Because dielectric constant indicates the strength of the relation between an electric field and polarization [13-16], if a polarization process loses its response, permittivity decreases [17,18]. What it can be seen from Fig. 3 is the increase of dielectric constant at higher wavelengths that shows the dispersive nature of NBT ceramics.

Fig. 3. Real (ε_r) and imaginary (ε_i) parts of dielectric constant for NBT nanostructured thin film vs. wavelength.

Information on the dispersion behavior of the optical constants of the material is crucial for designing and application of optical materials. Equations 3 and 4 are used to calculate the refractive index and extinction coefficient of the material

$$n(\omega)=\left[\frac{\varepsilon_r(\omega)}{2}+\frac{\sqrt{\varepsilon_r^2(\omega)+\varepsilon_i^2(\omega)}}{2}\right]^{1/2} \qquad (3)$$

$$\kappa(\omega)=\left[\frac{-\varepsilon_r(\omega)}{2}+\frac{\sqrt{\varepsilon_r^2(\omega)+\varepsilon_i^2(\omega)}}{2}\right]^{1/2} \qquad (4)$$

The results are shown in Fig.4. It is seen that both *n* and *k* show a similar trend of real and imaginary parts of dielectric function in the visible region and approach the maximum value around absorption edge (500 nm). However, for larger wavelengths, *k* follows a steady trend and reaches around 3 that implies very high attenuation of light in the mid and far infra-red (MIR & FIR) regions.
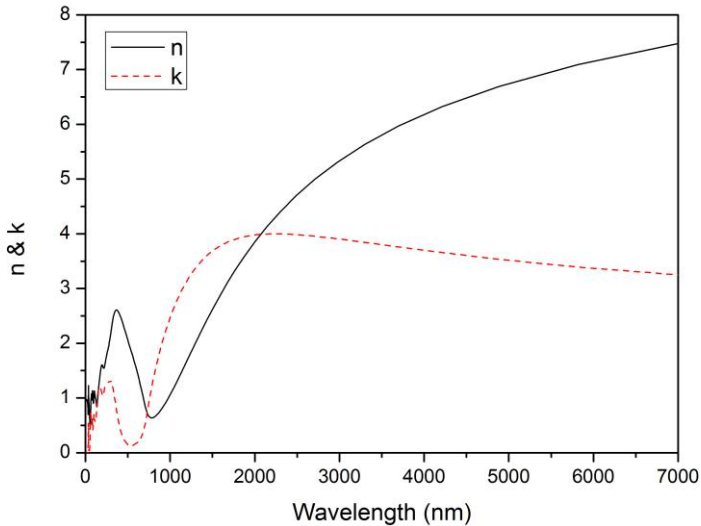
Fig. 4. Refractive index (n) and extinction coefficient (k) for NBT nanostructured thin film vs. wavelength.

The variation of extinction coefficient is generally assigned to the inelastic scattering of the electromagnetic waves in the semiconductor such as the Compton effect, photoelectric effect, pair production effect and so on [14]. On the other hand, the refractive index of the modeled thin film shows a very dispersive behavior in MIR and FIR while the values in Uv-visible region are consistent well with the reported data [1].

Fig. 5 illustrates the reflectivity of the modeled NBT thin film as a function of incident light wavelength. As it can be observed, the modeled thin film is rather less reflective in the visible region and the pertinent reflectivity increases

abruptly after 1000 nm. It is a normal expectancy of semiconductor materials to be more reflective beyond the plasma frequency. Due to resonance nature of the surface plasmon interactions with the incident photons, lots of photons with energies lower than plasma frequency will be reflected. Again, the reflectance spectrum is consistent with the reported data [1].

Optical conductivity is a powerful tool for investigation of the electronic states in a material. When a material is exposed to an external electric field a redistribution of charges occurs and currents are induced. Fig.6 shows the variation of the real and imaginary parts of optical conductivity, $\sigma = \dfrac{\alpha nc}{4\pi}$ (where c is the velocity of light) versus optical wavelength for the modeled NBT nanostructured thin film. As it is clear from Fig.6, the variation of optical conductivity takes places mostly in the Uv-vis region. This is due to the corresponding variations in the absorption coefficient of the compounds. A steady state can be seen for the rest of the spectrum.
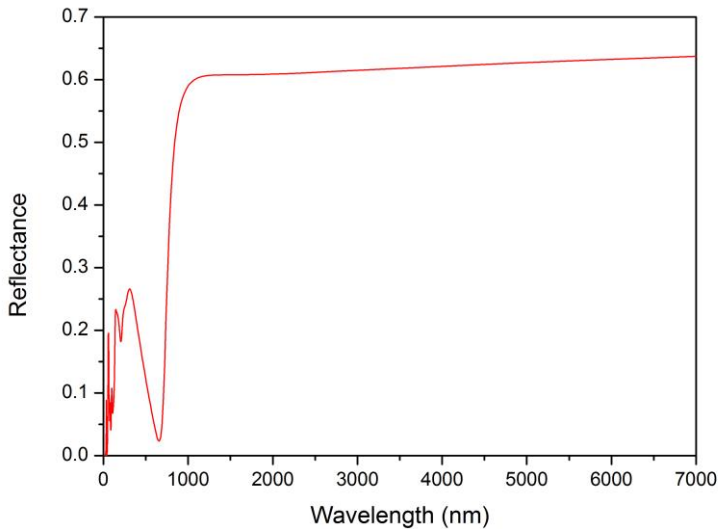
Fig. 5. Reflectance spectrum of NBT nanostructured thin film vs. wavelength.
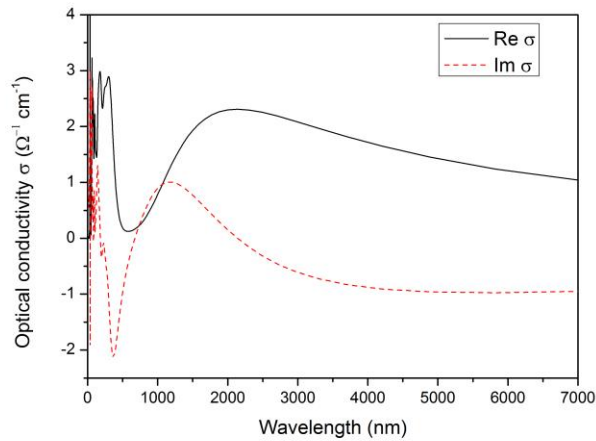
Fig. 6. Optical conductivity of NBT nanostructured thin film vs. wavelength.

Energy loss function $L(\omega)$ is an indication of the energy loss of the fast moving electrons traveling through the materials. Fig.7 exhibits the energy loss function of the modeled NBT nanostructured thin film as a function of wavelength. It is evident from the figure that the most energy loss occurs in the wavelengths lower than band edge as well just after band-to-band transition region between 500 and 1000 nm. Owing to non-reported experimental/theoretical results, no data were available to make comparison with our results.
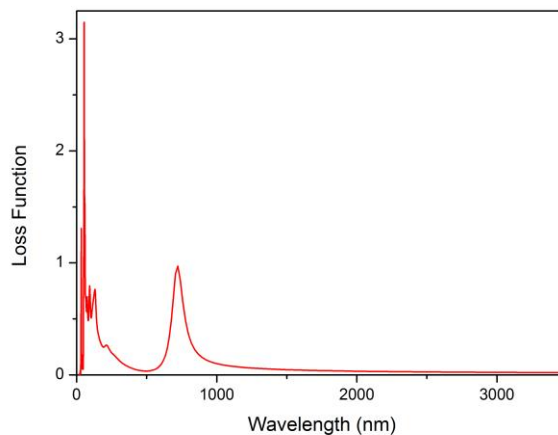
Fig. 7. Energy loss function of NBT nanostructured thin film vs. wavelength.

4. CONCLUSION

In brief, we studied the electronic and optical properties of NBT thin film with nanometer scale in rhombohedral phase using first–principle method. The input data for simulation were taken from the geometrically optimized structure in GGA. The band structure, energy bandgap and total density of states of the modeled thin film were calculated and compared with the available experimental and theoretical data. The evaluated optical bandgap of the simulated thin film was 2.1 eV that showed quite well consistency with the values calculated for bulk NBT structure. Trend of dielectric function of the constructed thin film was discussed. Meanwhile, the optical constants, the reflectivity and electron energy loss function of the material were also calculated and studied.

Acknowledgment

References

[1] M. Zeng, S. Wing, H. L. Wa Chan, *First-principles study on the electronic and optical properties of $Na_{0.5}Bi_{0.5}TiO_3$ lead-free piezoelectric crystal*. J. Appl. Phys. 107 (2010, 22 Feb.) 043513.
Available: https://aip.scitation.org/doi/full/10.1063/1.3309407

[2] Verma, A. Kumar Yadav, S. Kumar, V. Srihari, R. Jangir, H. K. Poswal ,S. Biring, S. Sen , *Enhanced energy storage properties in A-site substituted of $Na_{0.5}Bi_{0.5}TiO_3$ ceramics.* J. Alloys Compd. 797 (2019, 5 Jul.) 95–107.
Available: https://www.sciencedirect.com/science/article/pii/S0925838819311302

[3] H. Sankar Mohanty, T. Dam, H. Borkar, D. K Pradhan, K. K. Mishra, A. Kumar, B. Sahoo, P. K. Kulriya, C. Cazorla, J. F. Scott**,** D. K. Pradhan, *Structural transformations and physical properties of $(1-x)Na_{0.5}Bi_{0.5}TiO_3$-$xBaTiO_3$ solid solutions near a morphotropic phase boundary*. J. Phys.:Condens. Matter. 31 (2019) 075401.
Available: https://doi.org/10.1088/1361-648X/aaf405

[4] S.-E. Park, S.-J. Chung, and I.-T. Kim, *Ferroic phase transition in $Na_{0.5}Bi_{0.5}TiO_3$ crystals.* J. Am. Ceram. Soc. 79 (1996, May) 1290–1296.
Available: https://ceramics.onlinelibrary.wiley.com/doi/abs/10.1111/j.1151-2916.1996.tb08586.x

[5]   X. Yi, H. Chen, W. Cao, M. Zhao, D. Yang, G. Ma, C. Yang, J. Han, *Flux Growth and characterization of lead-free piezoelectric single crystal $[Bi_{0.5}(Na_{1-x}K_x)_{0.5}]$ TiO_3*. J. Cryst. Growth. 281 (2005, Aug.) 364–369. Available: https://www.sciencedirect.com/science/article/pii/S0022024805004136

[6]   M. K. Niranjan, T. Karthik, S. Asthana, J. Pan, U. V. Waghmare, *Theoretical and experimental investigation of Raman modes, ferroelectric and dielectric properties of relaxor $Na_{0.5}Bi_{0.5}TiO_3$.* J. Appl. Phys. 113 (2013, Apr.) 194106. Available: https://aip.scitation.org/doi/10.1063/1.4804940

[7]   K. Dorywalski, N. Lemée, B. Andriyevsky, R. Schmidt-Grund, M. Grundmann, M. Piasecki, M. Bousquet, T. Krzyzynski. Optical properties of epitaxial $Na_{0.5}Bi_{0.5}TiO_3$ *lead-free piezoelectric thin films: Ellipsometric and theoretical studies.* App. Surf. Sci. 421 (2017, Nov.) 367-372. Available: https://www.sciencedirect.com/science/article/pii/S016943321631947X

[8]   B. Delley, *From molecules to solids with the $DMol^3$ approach*. J. Chem. Phys. 113 (2000, Oct.) 7756–7764. Available: https://aip.scitation.org/doi/10.1063/1.1316015

[9]   F. A. Hamprecht, A. J. Cohen, D. J. Tozer, N. C. Handy, *Development and assessment of new exchange-correlation functionals*. J. Chem. Phys. 109 (1998, Jul.) 6264–6271. Available: https://aip.scitation.org/doi/10.1063/1.477267

[10] H.J. Monkhorst, J.D. Pack, *Special points for Brillouin-zone integrations*. Phys. Rev. B 13 (1976, Jun.) 5188–5192. Available: https://journals.aps.org/prb/abstract/10.1103/PhysRevB.13.5188

[11] G. O. Jones, P. A. Thomas, *Investigation of the structure and phase transitions in the novel A-site substituted distorted perovskite compound $Na_{0.5}Bi_{0.5}TiO_3$.* Acta Crystallogr. B 58 (2002, Apr.) 168–178. Available: http://journals.iucr.org/b/issues/2002/02/00/os0082/rtvsup.html

[12] R. Bujakiewicz-Koroska, Y. Natanzon, *Determination of elastic constants of $Na_{0.5}Bi_{0.5}TiO_3$ from ab initio calculations.* Phase Transit. 81 (2008, Dec.) 1117–1124. Available: https://www.tandfonline.com/doi/full/10.1080/01411590802460833

[13] H. Izadneshan, G. Solookinejad, *Effect of annealing on physical properties of Cu_2ZnSnS_4 (CZTS) thin films for solar cell applications.* JOPN. 3 (2) (2018, Spring) 19-28. Available: http://jopn.miau.ac.ir/article_2861.html

[14] M. Borhani Zarandi, H. Amrollahi Bioki, *Effects of cobalt doping on optical properties of ZnO thin films deposited by sol-gel spin coating technique*. JOPN. 3(2) (2019, Autumn) 33-44.
Available: http://jopn.miau.ac.ir/article_2572.html

[15] S. Manouchehri, J. Zahmatkesh, M. H. Yousefi, *Substrate effects on the structural properties of thin films of lead sulfide.* JOPN. 3(2) (2019, Spring) 1-18. Available: http://jopn.miau.ac.ir/article_2860.html

[16] Z. Dehghani Tafti, M. Borhani Zarandi, H. Amrollahi Bioki, *Thermal annealing influence over optical properties of thermally evaporated SnS/CdS bilayer thin films.* JOPN. 4(1) (2019, Winter).
Available: http://jopn.miau.ac.ir/article_3387.html

[17] M. Cheraghizadeh, *Optoelectronic properties of PbS films: Effect of carrier gas*. JOPN. 4(2) (2019, Spring).
Available: http://jopn.miau.ac.ir/article_3474.html

[18] Y. Abed, F. Mostaghni, *Polarizability and hyperpolarizability of Schiff base salen-H2 as judged as UV-vis spectroscopy and simulation analysis*. JOPN. 3(1) (2018, Winter) 27-40.
Available: http://jopn.miau.ac.ir/article_2821.html